DESIGN AND CHARACTERIZATION OF TWO-JUNCTION TUNING CIRCUITS FOR SUBMILLIMETER SIS MIXERS

M.C. Gaidis, M. Bin, D. Miller, J. Zmuidzinas
George W. Downs Laboratory of Physics, 320-47
California Institute of Technology, Pasadena, CA 91125

H.G. LeDuc, J.A. Stern
Jet Propulsion Laboratory, 302-231, Pasadena, CA 91109

Abstract

We report on the continuing development of submillimeter quasi-optical slot antenna SIS mixers which use two-junction tuning circuits [1]. The mixers use 10 kA/cm^2 Nb/Al-Oxide/Nb junctions and Nb wiring, and have generated DSB receiver noise temperatures around $5h\nu/k_B$ to 700 GHz, and $16h\nu/k_B$ (620 K) at 798 GHz. We present Fourier-transform spectrometer (FTS) measurements and heterodyne measurements on several such devices. In general, the measured response at frequencies below the gap of Nb is in good agreement with the predicted performance.

Introduction

SIS mixers with Nb-trilayer tunnel junctions offer excellent performance at frequencies below 800 GHz, and should perform competitively at frequencies as high as 1.4 THz [2-5]. Our goal is to develop a suite of ultra-low-noise SIS mixers which cover frequencies from ≈ 400 GHz to more than 1 THz.

At frequencies below the Nb gap (< 700 GHz), existing devices perform quite well [6], but further improvements in noise temperatures remain important. In addition, it is quite useful to be able to predict device performance given the design parameters. One can then optimize the device design for a particular frequency band, and confirm that we indeed understand the physics of the device. Progress in the design and operation of devices in this frequency range is presented below.

At frequencies above the Nb gap, RF photons can break Cooper pairs, resulting in greater signal loss and higher receiver noise temperatures. The loss is particularly important in the slender microstrip lines used to resonate the junction capacitance and to transform the antenna impedance down to the RF junction impedance. However, the actual coupling of radiation into Nb junctions above the gap should still be reasonably efficient -- more than 30% at 800 GHz [7]. In addition to RF loss, one is also affected by increased dispersion at frequencies near the gap. The Nb microstriplines have therefore been carefully designed to ensure the desired bandpass is achieved. We demonstrate for the first time that all-Nb SIS receivers can have substantially better performance than GaAs Schottky receivers for the astronomically important CI ($^3P_2 - {}^3P_1$) and CO (7–6) transitions near 810 GHz.

Receiver Configuration

Since waveguide mixers become difficult to construct at short submillimeter wavelengths, we have adopted a quasi-optical approach. Here, lenses take the place of waveguide horns, and the incoming radiation is collected by a planar antenna on the SIS mixer substrate [8]. This offers several other advantages, such as on-chip broad-band

lithographic tuning elements, straightforward scaling to yet higher frequencies, and natural adaptation to focal-plane imaging arrays.

A macroscopic view of the receiver is presented in Figure 1; the microscopic description of the mixer chip follows in the next section. The local oscillators (LO) used for our measurements are compact, solid-state, tunable Gunn oscillators with varactor multipliers. The signal and LO are combined with 10 or 25 μm mylar beamsplitters, which couple approximately 8% or 23% (92% or 77%) of the LO (signal) power into the device, respectively, at 810 GHz. Low LO power levels available from our oscillator chain at the higher frequencies often dictates the use of the thicker (25 μm) beamsplitter. Although convenient, the beamsplitter can significantly increase the measured receiver noise temperature.

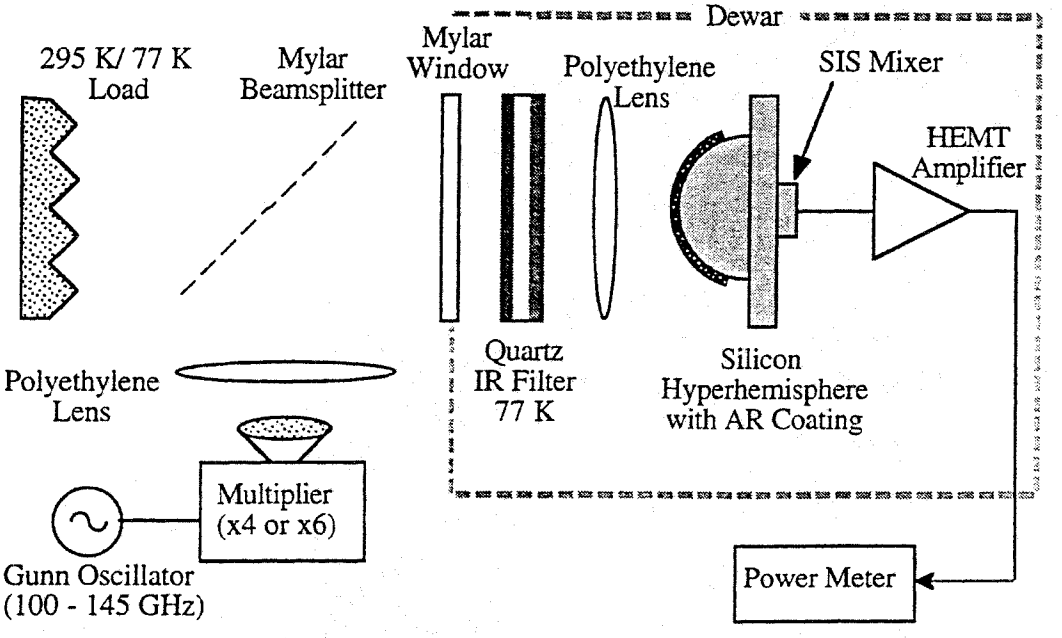

Figure 1: Simplified receiver layout.

The combined signal and LO travel into the vacuum dewar through a 25 μm mylar window at room temperature, followed by a 2.5 mm thick, z-cut quartz IR filter at 77 K. In the 800 GHz band experiments to be discussed below, both sides of this quartz had an additional antireflection (AR) coating which was optimized for ≈ 820 GHz. This coating consists of a ≈10 μm thick black Xylan primer sprayed on the quartz, followed by clear Teflon FEP to the thickness required for optimal AR performance [9]. The window and coating withstand repeated thermal cycling, and are quite durable. We have not measured the IR transmission properties, but we note that the dewar helium hold time is limited by thermal conduction along the electronic wiring, rather than radiation through the optical path. For a similar IR filter, with AR coating optimized for 590 GHz, the RF loss (including reflection and absorption loss) was measured at less than 5% at 690 GHz. The normal to the quartz IR filter used in the 800 GHz band experiments is also tilted at a ≈ 5° angle with respect to the beam in an effort to suppress Fabry-Perot resonances. (In the 550 GHz band measurements, the quartz IR filter is perpendicular to the beam.)

A polyethylene lens and a silicon hyperhemisphere, AR coated with alumina-loaded epoxy [6,10], transform the ≈ F/17 input beam to match the broad pattern of the twin-slot

planar antenna. In the near future, we will replace the polyethylene lens with teflon-coated quartz, which should give ≈ 10% gain in coupling efficiency.

The IF output from the mixer is fed to a low-noise amplifier which has a bandwidth of ≈ 1.25 – 1.75 GHz and a specified noise temperature of 3 K [11]. The amplifier output is sent to room temperature amplifiers and a diode detector which measures the total power in the 500 MHz IF bandwidth.

Mixer Design and Fabrication

The detailed design of the twin-slot planar antenna and the two-junction SIS mixer tuning circuit has been presented elsewhere [1,6]. Figure 2 is a diagram representative of the mixers used in this work. The present mixers are quite similar to earlier designs, except for several right-angle bends in the transformer sections. These bends allow us to better optimize the impedance match between the antenna (≈ 30 Ω) and the tunnel junctions (≈ 10 Ω). We have written a computer program to simulate and optimize the device design. Our circuit model includes the frequency-dependent impedance of the antennas, striplines, and tunnel junctions. The properties of the superconducting microstrip lines are calculated using our previously described method [8], which includes the frequency-dependent surface impedance given by the Mattis-Bardeen theory in the local limit. Future work on the simulator will include RF loss in the antenna.

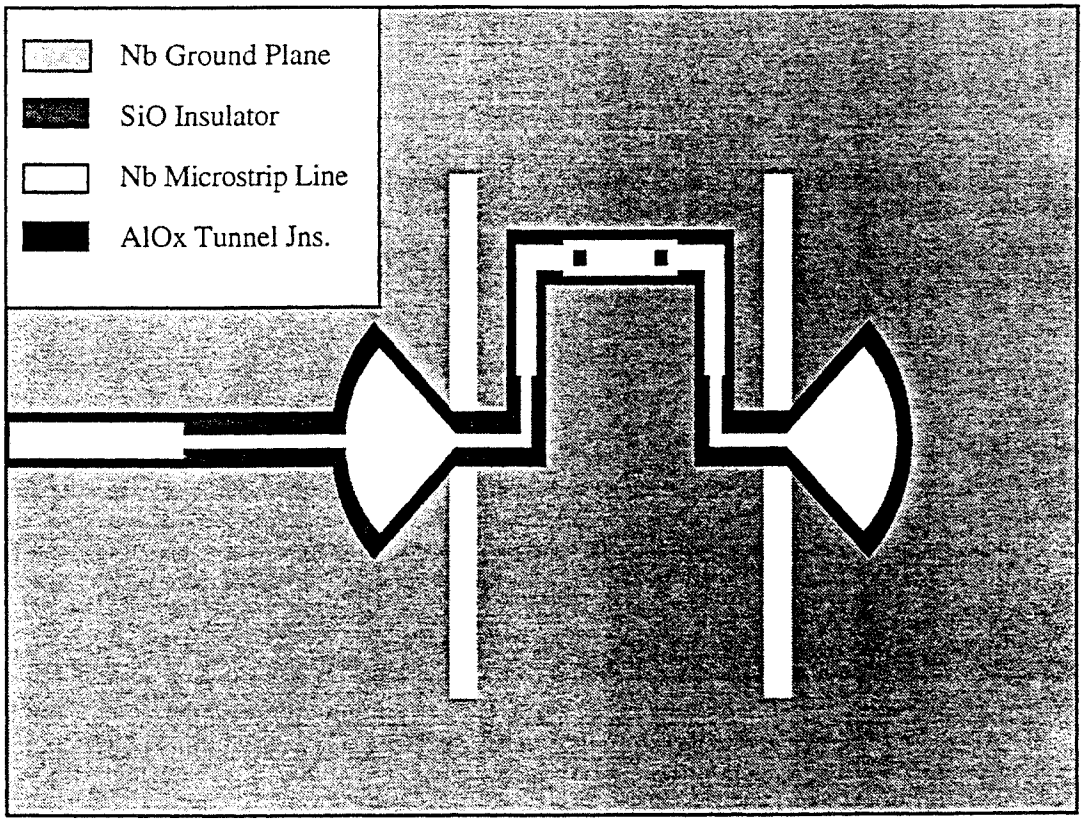

Figure 2: Twin-slot antenna, two-junction SIS mixer design (top view).

The use of antisymmetrically driven tunnel junction pairs simplifies the inductive tuning necessary to resonate the junction capacitance. The resonating inductance for each junction is simply one-half the total inductance joining the two junctions, as the antisymmetric feed creates a virtual ground halfway between the two junctions [1]. Because the junctions are defined in the same lithographic step, misalignment between lithography layers cannot significantly affect the tuning inductance. A misalignment will primarily produce a minor phase difference between the two slot antennas, which results in a very slightly tilted beam -- approximately 2° per μm misalignment, compared to the beam FWHM of 48°.

The low antenna impedance promotes good impedance matching to even relatively low-resistance tunnel junctions. Therefore, we design with junction areas between 1.2 μm^2 and 2.3 μm^2, and can utilize JPL's all-optical-lithography junction fabrication process [1,8]. These large area junctions are easier to fabricate than e-beam devices, can be less sensitive to static discharge, and offer adequate bandwidths ($\omega RC \approx 7$ at 700 GHz). One drawback of large junctions is the need for higher LO power -- as much as a factor of 4 more than for typical e-beam defined junctions.

Device designs were generated with the simulation program to cover the frequency range from ≈ 400 GHz to ≈ 800 GHz. To allow for parameter variation, particularly in the junction areas and specific capacitance, we have included three different nominal junction sizes (1.2 μm^2, 1.7 μm^2, and 2.3 μm^2) for each tuning structure design. Design specifications for the two devices discussed below are presented in Table 1. Note that the design of the 1995 mixers is also adjusted to reduce overall capacitance for broadband IF output (to > 4 GHz).

Parameter	Device 623 (1993)	Device 73 (1995)
Ground Plane	2000 Å Nb	2000 Å Nb
Wiring	2000 Å Nb	2000 Å Nb
RF Choke (IF Output)	Nb microstrip	Nb coplanar
90° Radial Stub Radius	29 μm	36 μm
Slot Antenna Size	154 μm x 7.7 μm	133 μm x 6.7 μm
Slot Spacing	77 μm	67μm
First Transformer Section (WxL)	3 μm x 25 μm	5.8 μm x 15 μm
Second Transformer Section (WxL)*		3.3 μm x 15 μm
SiO Thickness: Transformer Microstrip	2000 Å	4000 Å
Junction Area	0.9 μm^2	2.3 μm^2
Junction Specific Capacitance	85 fF/μm^2	65 fF/μm^2
Junction Resistance–Area Product	15.6 Ω μm^2	26.1 Ω μm^2
Inductor (Between Jn. Centers) (WxL)	6 μm x 22.4 μm	5 μm x 7 μm
SiO Thickness: Inductor Microstrip	2000 Å	2000 Å

*For the 623 device, only one transformer section was used. Neither of these devices utilized right-angle bends in the transformer section. All devices used a 2.5 micron length of microstrip (width equal to inductor width) to connect the last transformer with the inductor.

Table 1: Design parameters for two representative devices.

Receiver Performance

Receiver response as a function of frequency was measured using an FTS system (built in-house) using the mixer as a direct detector. Although we cannot yet reliably measure the absolute response using the FTS, the *shape* of the relative response vs. frequency is quite reliable. The absolute response of different devices is best compared by performing heterodyne measurements. We find that the variation of the noise temperature with frequency correlates well with the response measured on the FTS, so that we can rely heavily on FTS data to select useful devices from a given fabrication run.

Figure 3 illustrates the accuracy with which we can predict mixer response at present. The simulation curves give the fraction of the power received by the antenna which is dissipated in the junction resistances. The vertical scale of the FTS data is arbitrarily adjusted to give the best match to the simulation. This is considered valid, as coupling differences between FTS runs should be frequency-independent.

In general, the agreement is quite good, given the nonidealities present in the measurement: strong water absorption lines at 557 and 752 GHz, and Fabry-Perot resonances from the quartz IR filter spaced approximately 50 GHz apart. (The only correction for optics in the data is for the efficiency of the mylar beamsplitter in the FTS. The frequency-dependent quantum responsivity of the detector, $\propto 1/\nu$, is also corrected for in the figures.) The FTS data presented for device "623" was obtained with a poor-quality black polyethylene A/R coating on the IR filter, and shows considerable Fabry-Perot resonances. The "73" device results are not so affected, presumably because of the more effective teflon A/R coating discussed above, and because of a 10° angle to the IR filter. The deviation between FTS data and simulation at higher frequencies is not well understood at present, but can be partially attributed to antenna losses which were not included in the simulation.

More than ten different device designs have been tested in this manner to date, and all agree with simulations to the degree shown in Figure 3, thus indicating that the simulation method is reasonably reliable. For a given fabrication run, the junction capacitance is the only variable parameter. When this is fixed by FTS data from one device, the FTS data from remaining devices in the batch will match the simulations with no fittable parameters (other than the arbitrary amplitude scaling). Junction capacitance has been our largest uncertainty, possibly being affected by small amounts of high-dielectric-constant Nb oxides in the tunnel barrier. It appears, however, that a recent change in the fabrication process -- using DC sputtering for the Al junction barrier layer, rather than RF sputtering -- has resulted in somewhat more reproducible results. The typical junction specific capacitance for the new devices is ≈ 65 fF/μm^2. This is determined from FTS measurements of the device bandpass, as compared with simulations (below the Nb gap), and is adusted for junction area variations through the use of test die on the device wafer. The (minor) observed variations in junction resistance have only a small effect on the overall bandwidth.

The rather unconventional shapes of the response curves have different origins for the two devices. The older "623" design (1993) was originally optimized to give relatively flat, >90% response in the 600 to 700 GHz band. However, the capacitance of the fabricated junctions appears to be $\approx$ 25% higher than assumed for the design, and this, combined with an error in the microstrip circuit design, has skewed the passband and shifted it to lower frequency. The theoretical curve shown in Figure 3 has been adjusted for these deviations. Even with the nonideal bandpass, the device exhibits respectable heterodyne noise temperatures, as presented below. The more recent "73" design was optimized for a center frequency of 750 GHz. The design optimization incorporates response above the Nb gap, where losses are very important. This explains the relatively low peak response and the odd shape of the theoretical curve. This 1995 photomask design also includes devices optimized for passbands of 400 – 500 GHz, 500 – 600 GHz, and 600 – 700 GHz. These devices have been designed for high response (>90%), flat

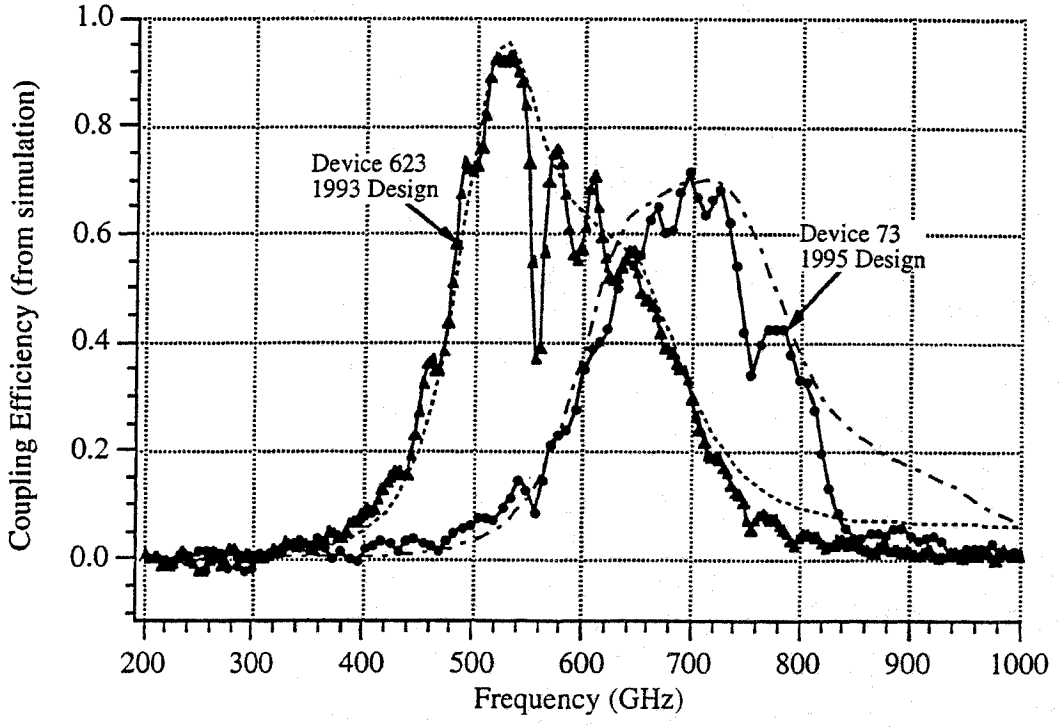

Figure 3: FTS measured response (solid lines) vs. mixer simulation (dashed lines) for two representative devices.

passbands. Preliminary measurements on the 600 – 700 GHz device are quite encouraging.

We have measured the noise temperatures of several devices, including those in Figure 3, using the Y-factor method. Our noise temperatures are referred to the input of the beamsplitter; unless otherwise noted, no corrections have been made for the beamsplitter or other optical losses. Figure 4 shows the DC current-voltage characteristics of the "73" device characterized in Figure 3. The pumped (798 GHz) and unpumped I-Vs are shown for a bath temperature of 4.2 K. The photon step from the nonlinearity at $V = -2\Delta/e \approx -2.85$ mV appears at $V \approx +0.45$ mV, as expected from the 798 GHz LO input ($hv/e \approx 3.3$ mV). Also shown in Figure 4 are the total IF output power in a 500 MHz bandwidth when room temperature and 77 K absorbers are placed at the receiver input. The curves are relatively smooth, indicating good suppression of Josephson noise. With no mechanical tuning elements -- simply adjustment of the magnetic field, bias, and LO power -- this device gives a DSB receiver noise temperature of 787 K at the 798 GHz LO frequency.

Figure 5 displays receiver noise temperatures as a function of frequency for several of our best devices. Interesting to note from the plot are the noise temperatures of the "73" device when cooled to 2.5 K. The noise temperatures decrease by as much as 100 K, in part due to a slightly higher Nb gap at the lower temperatures, and the correspondingly lower stripline losses. The lower ambient temperature also decreases the shot noise from the dark current, which is ≈ 40% of the total (pumped) bias current at 4.2 K. Receiver noise temperatures are adversely affected by the relatively low output power typical of our LO chain configuration, and the situation is further degraded by our power-hungry large junction areas (2.25 μm^2 for this particular device). The use of thicker beamsplitters to couple in more LO power does not improve the receiver noise temperature, as a greater portion of the signal is reflected away from the mixer. The device would offer

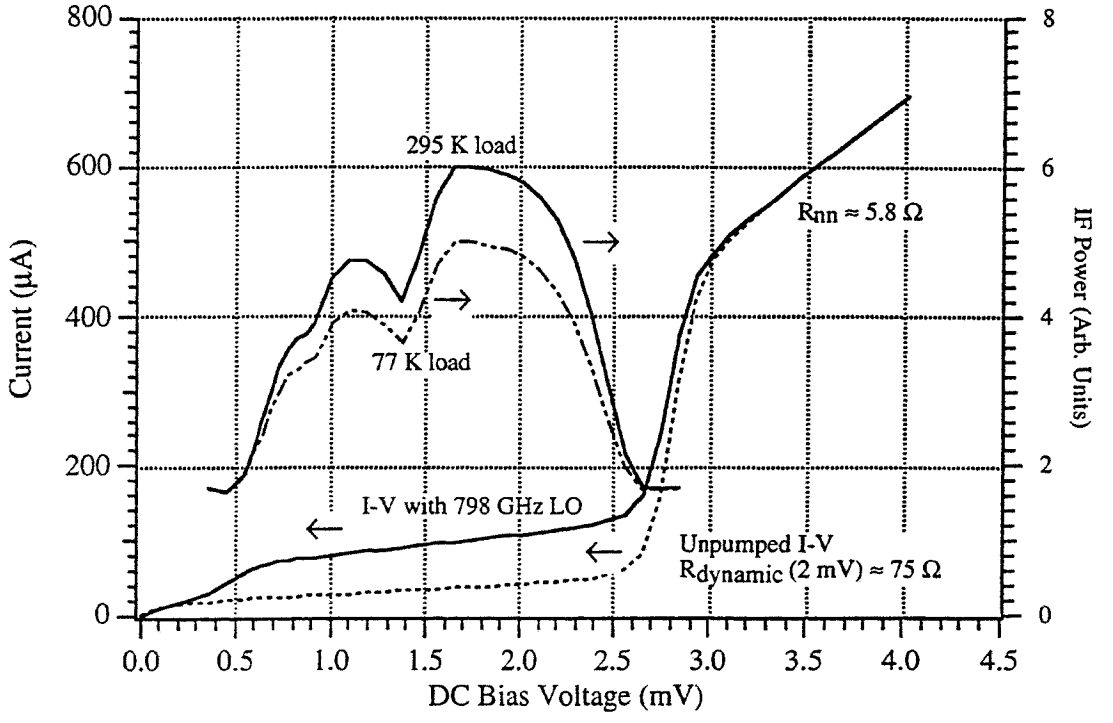

Figure 4: Current vs. voltage trace and IF power vs. voltage bias for device "73" at 4.2 K. The LO frequency is 798 GHz, and the DSB receiver noise temperature is 787 K.

significantly lower noise temperatures if a stronger LO source with thinner beamsplitter were employed. (Correcting for present beamsplitter losses would improve the 798 GHz, 2.5 K receiver noise temperature from 617 K to below 450 K.)

To our knowledge, the (uncorrected) results presented in Figure 5 are the best reported to date for any broadband heterodyne receiver at 800 GHz. To highlight the usefulness of our low-noise SIS receiver, we compare with state-of-the-art Schotty corner-cube receivers -- offering DSB receiver noise temperatures no better than 1500 K (*after* correcting for the ≈ 50% corner-reflector antenna efficiency) [12].

Conclusion and Outlook

We have demonstrated quasi-optical low-noise SIS receivers with *predictable* performance at frequencies up to ≈ 800 GHz. The measured receiver noise temperatures are low enough to perform exciting astronomy in the $\lambda = 350$ μm atmospheric window. Our device simulation program can accurately predict the experimentally observed performance, giving us the ability to reliably design broadband, high sensitivity devices over our frequency range of interest, 400 – 800 GHz. Preliminary results on other devices in the series further supports this claim, giving expected bandwidths, and respectable receiver noise temperatures (for example, 180 K DSB at 690 GHz).

We have initiated a program to replace the Nb antenna and stripline with lower loss normal-metal Al films. We expect these devices to have useful response at frequencies exceeding 1 THz. Reuter-Sondheimer theory has been used to predict the surface impedance of Al in this regime of the anomalous skin effect. The Al device response does not approach that of lower frequency fully-superconducting devices, but we expect to achieve receiver noise temperatures below 10 hν/k at 1 THz. We believe the Al device

predictions to be reasonably accurate, judging from experiments with non-optimized Al-wiring devices at lower frequencies: the existing Nb-wiring device masks were used to establish the Al-wiring device fabrication process, and the resulting devices were tested on our FTS. Although these devices have 550 – 650 GHz bandwidths, our success with all-Nb devices above the Nb gap indicates that it is reasonable to expect Al-wiring devices will extend the useful frequency range of our mixers beyond 1 THz.

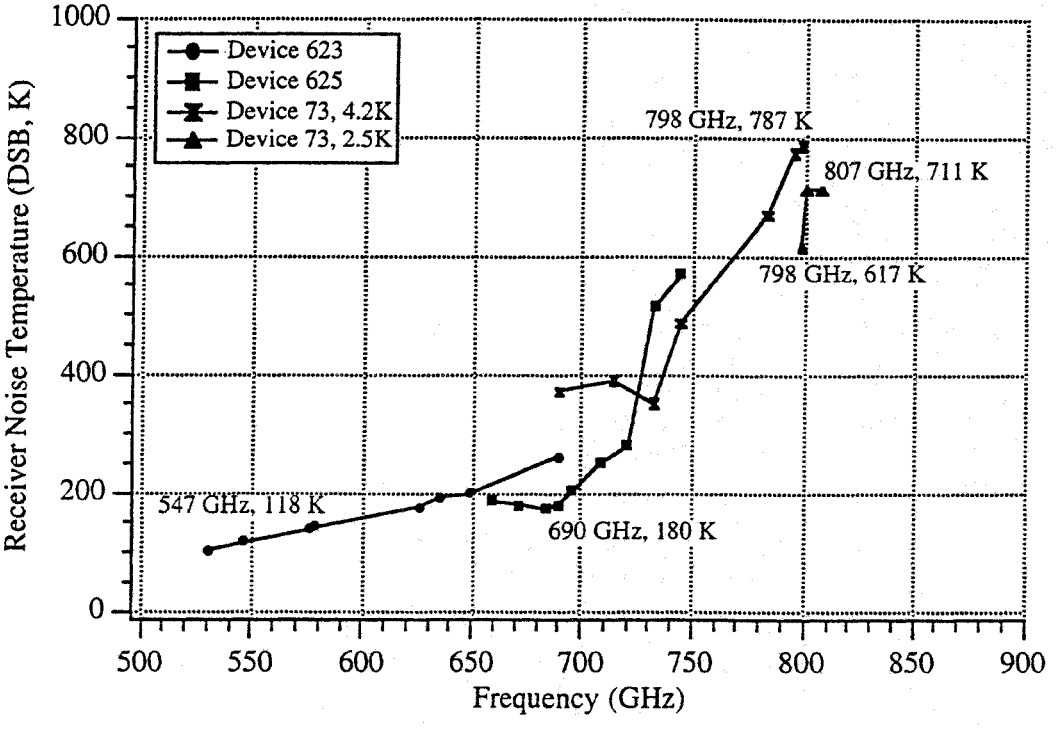

Figure 5: Noise temperatures of selected devices. $2\Delta/h \approx 700$ GHz for our Nb films.

Acknowledgements

We thank N.G. Ugras, A. Clapp, J. Ward, J. Kooi, R. Schoelkopf, and T. Büttgenbach for their contributions to the laboratory work and for helpful advice. This work was supported in part by grants from NASA (NAGW-107 and NAG2-744), NASA/JPL, and a NSF PYI grant to J.Z. The junction fabrication was performed at the Center for Space Microelectronics Technology, Jet Propulsion Laboratory, California Institute of Technology and was sponsored by the National Aeronautics and Space Administration, Office of Space Access Technology.

References

[1] J. Zmuidzinas, H.G. LeDuc, J.A. Stern, and S.R. Cypher, "Two Junction Tuning Circuits for Submillimeter SIS Mixers," *IEEE Trans. Microwave Theory Tech.* **42**, 698-706 (1994).

[2] G. DeLange, C.E. Honingh, J.J. Kuipers, H.H.A. Schaeffer, R.A. Panhuyzen, T.M. Klapwijk, H. Van de Stadt, and M.M.W.M. de Graauw, "Heterodyne Mixing with Nb Tunnel Junctions Above the Gap Frequency," *Appl. Phys. Lett.* **64**, 3039-3041 (1994).

[3] D. Winkler and T. Claeson, "High Frequency Limits of Superconducting Tunnel Junction Mixers," *J. Appl. Phys.* **62**, 4482-4498 (1987).

[4] M.J. Wengler and D.P. Woody, "Quantum Noise in Heterodyne Detection," *IEEE J. Quantum Electronics* **23**, 613-622 (1987).

[5] W.C. Danchi and E.C. Sutton, "Frequency Dependence of Quasiparticle Mixers," *J. Appl. Phys.* **60**, 3967-3977 (1986).

[6] J. Zmuidzinas, N.G. Ugras, D. Miller, M. Gaidis, H.G. LeDuc, and J.A. Stern, "Low-Noise Slot Antenna SIS Mixers," to appear in the proceedings of the Applied Superconductivity Conference, Boston, MA, 1994.

[7] R. Pöpel, "Electromagnetic Properties of Superconductors," pp. 44-78 in V. Kose, ed., Superconducting Quantum Electronics, Springer-Verlag: Berlin, 1989.

[8] J. Zmuidzinas and H.G. LeDuc, "Quasi-optical Slot Antenna SIS Mixers," *IEEE Trans. Microwave Theory Tech.* **40**, 1797-1804 (1992).

[9] Thermech Engineering Corp, 1773 W. Lincoln Ave, Bldg. K, Anaheim, CA 92801.

[10] Janos Technology, Inc., HCR #33, Box 25, Route 35, Townshend, VT 05353-7702.

[11] Berkshire Technologies, Inc., 5427 Telegraph Ave., Suite B2, Oakland, CA 94609; model L-1.5-30HI.

[12] A.I. Harris, J. Stutzki, U.U. Graf, and R. Genzel, "Measured Mixer Noise Temperature and Conversion Loss of a Cryogenic Schottky Diode Mixer Near 800 GHz," *Int. J. Infrared and Millimeter Waves* **10**, 1371-1376 (1989).